Electronic structure of liquid transition metals studied by time resolved photoelectron spectroscopy

2000 J. Phys.: Condens. Matter 12 A9

(http://iopscience.iop.org/0953-8984/12/8A/302)

J. Phys.: Condens. Matter **12** (2000) A9–A18. Printed in the UK PII: S0953-8984(00)07657-8

Electronic structure of liquid transition metals studied by time resolved photoelectron spectroscopy

P Oelhafen, R Wahrenberg and H Stupp†

Institute of Physics, University of Basel, Klingelbergstrasse 82, CH-4056 Basel, Switzerland

Received 30 June 1999

Abstract. The electronic structure of liquid transition metals has been studied by time resolved photoelectron spectroscopy. Distinct changes in the valence band structure across the solid–liquid phase transitions have been observed for Pd, Mo and W. In the case of Pd the changes on melting are caused by a change in the photoemission process itself. For Nb, Mo, Ta and W we suggest a change in the atomic short range order from the bcc structure to an fcc-like short range order in the liquid state which causes a marked change in the valence band spectra of Mo and W due to the filling up of the pronounced gap in the density of states near the Fermi level. The measurements show that time resolved photoelectron spectroscopy can be used to study high temperature oxidation processes on the microsecond time scale.

1. Introduction

Ultraviolet photoelectron spectroscopy (UPS) has been applied in order to study the electronic structure of metals now for four decades [1, 2]. Almost from the very beginning, attempts have been made to apply the method for liquid metals as well [3–5]. However, these early experiments performed on solid and liquid metals suffered quite often from contaminated surfaces and therefore the valence band spectra did not reflect the intrinsic valence electron structure of the metals under investigation. Later on, x-ray photoelectron spectroscopy (XPS) [6] became a quite common technique which enabled us to test unambiguously the cleanliness of sample surfaces. However, compared with corresponding studies on solid metals there was no standard cleaning procedure for liquid metals in order to obtain atomically clean surfaces until the mid-eighties.

With the introduction of the *wire cleaner device* [7] the study of *all* the metals in the periodic table with vapour pressures below some 10^{-4} Pa at the melting point became feasible and has been applied routinely for combined UPS, XPS, photoelectron spectroscopy with synchrotron radiation and Auger electron spectroscopy measurements (AES) [8–17]. These second generation steady state electron spectroscopy experiments are feasible in the case of some 20 elements in the periodic table. The study of the remaining elements (such as *all* the transition elements with the exception of Au) is hindered by a fundamental limitation in electron spectroscopy: the photoelectrons have to reach the detector after travelling through the spectrometer without collisions with residual gases or vapour from the liquid sample. It is this condition which restricts the study of liquid metals to vapour pressures below 10^{-4} Pa at the melting point for liquid metals.

† Permanent address: LASER 2000, Argelsrieder Fel 14, D-82234 Wessling, Germany.

0953-8984/00/SA0009+10$30.00

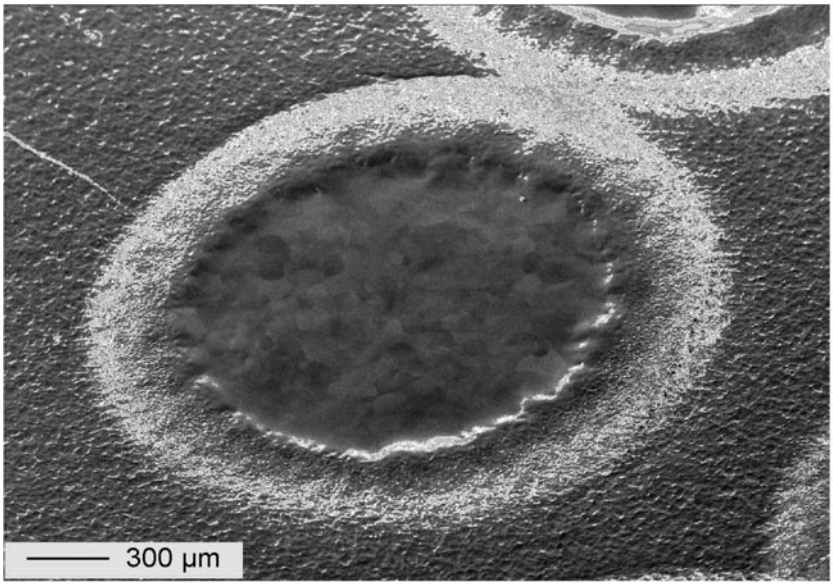

Figure 1. Scanning electron microscopy image of the repeatedly molten circular area on top of the Ta sample. The diameter of the spot is about 1.5 mm. The conservation of an ideally flat surface during the whole measuring process with about 10^5 melting–solidification cycles strongly depends on the choice of two parameters: base temperature and laser pulse energy density.

In order to circumvent the vapour pressure limit and to reach extremely high temperatures a new dynamic experimental method has been developed: surface heating by laser pulses combined with time resolved photoelectron spectroscopy (TR-PES) [18–21]. This method enables third generation experiments on high melting transition metals such as W in the liquid state [22] and measurements on liquid metals with corresponding equilibrium vapour pressures of 100 Pa have been performed. No vapour pressure limit has been observed so far for this new dynamic method.

In this paper we present new data on the liquid transition metals Nb and Ta and discuss them in the context of previously obtained data from Pd, Mo [23] and W [22].

2. Time resolved photoelectron spectroscopy

The valence band and core level spectra have been recorded on a modified VG ESCA-LAB 210 spectrometer. The samples have been preheated by a conventional ohmic heater to an appropriate base temperature in order to avoid a surface roughening by the multiple phase transitions in the course of the experiment. The sample surface quality has been observed directly by means of a CCD microscope camera during the experiment and has been checked additionally by scanning electron microscopy (SEM) after the photoelectron spectroscopy (PES) experiment. So far, no generally valid recipe for the choice of the two parameters, base temperature and laser energy density, has been found in order to maintain an optimal flat surface during the multiple melting–solidification processes necessary to obtain an acceptable statistics in the photoelectron spectra. In addition, polycrystalline samples and single crystals with various orientations have been tested in our experiments. However, no clear influence on surface roughening has been found. The sample surface temperature has been determined by a fit of the Fermi–Dirac function to the Fermi edge in the valence band spectrum. This

procedure is applicable in those cases where the density of states is only moderately changing across the Fermi energy and has an accuracy of about ±200 K. Further information on the sample temperature as a function of time has been obtained by calculating the light absorption and heat diffusion numerically. In addition, the laser energy required to melt the sample surface has been observed by means of the microscopy camera. Figure 1 shows an ideal spot on top of a Ta sample.

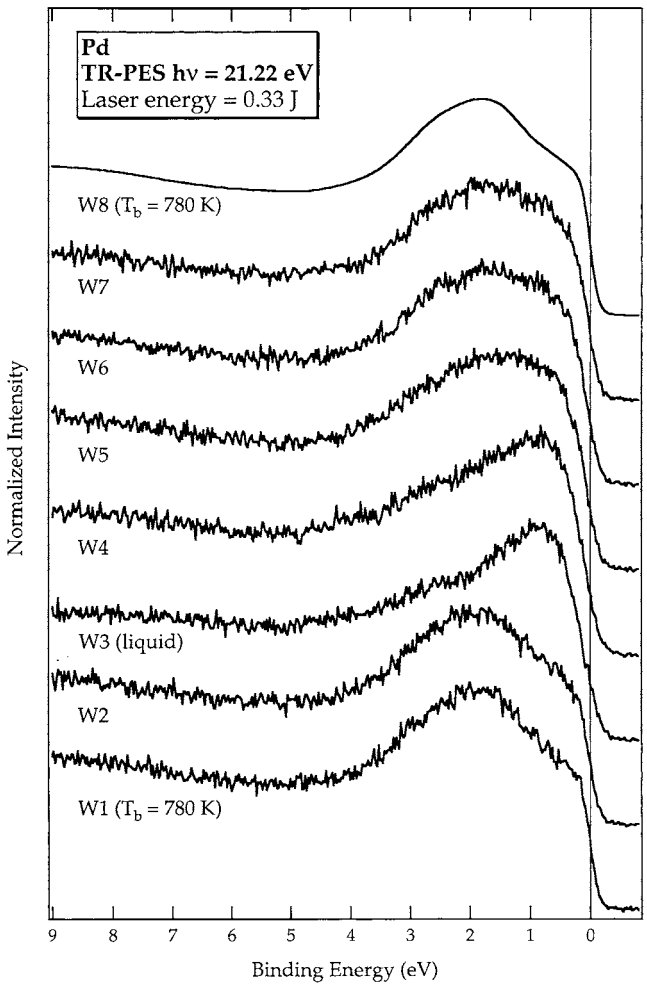

Figure 2. TR-PES valence band spectra of Pd during laser pulse heating with a pulse energy of 0.33 J/pulse and a base temperature of 780 K. The spectrum measured in time window W3 corresponds to the liquid phase. The eight time windows W1–W8 are defined in the text.

A flash lamp pumped dye laser (Cynosure) with a wavelength of 595 nm, a repetition rate of 10 cps and a spot diameter of about 1.5 mm has been used for surface heating of the sample (for technical details see [19]). The pulse width amounts to 2.1 μs (full width at half maximum) and the maximum pulse energy is of the order of 1.2 J. Photoelectrons are either excited by an He resonance lamp with a photon energy of $h\nu = 21.2$ eV and a spot diameter of 0.8 mm on the sample (modified Leybold/SPEC UVS 10/35 source) or by monochromatized Al Kα ($h\nu = 1486.6$ eV) radiation with an x-ray spot of 0.8 mm on the sample. In the present work

the latter has been used in order to characterize the cleanliness of the sample surface and no contaminants have been detected in the liquid state of the elements presented here. However, we will show below for the example of Nb that time resolved XPS measurements are feasible to monitor the evolution of a surface oxide layer. In combination with time resolved UPS measurements the dynamics of surface oxidation can be studied with a time resolution of the order of microseconds. All photoelectron spectra presented here are shown as recorded by the spectrometer, i.e. without any further data treatment.

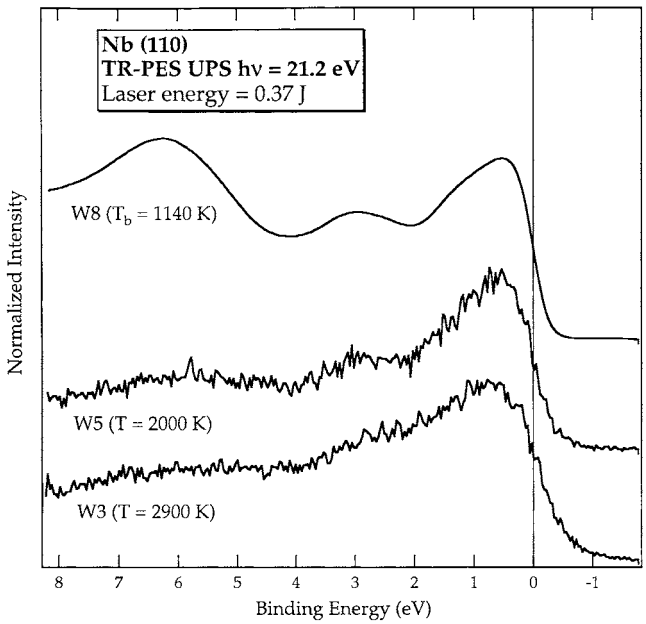

Figure 3. TR-PES valence band spectra of Nb: the liquid phase measured at 2900 K; the solid phase measured at 2000 K and at 1140 K. Time windows W3, W5 and W8 start 2 μs, 6 μs and 5 ms after the start of the laser pulse, respectively, and the corresponding widths are 2 μs for W3 and W5 and 2 ms for W8.

3. Results from Pd, Nb, Ta, Mo and W across the solid–liquid phase transition

Figure 2 shows UPS valence band spectra of Pd measured in eight different time windows with defined starting times with respect to the laser pulse. Time windows W1–W7 cover a time range of 14 μs, and have a duration of 2 μs each and W1 starts 2.3 μs before the onset of the laser pulse. Time window W8 starts 5 ms after the onset of the laser pulse and has a duration of 2 ms. As a consequence, the spectra measured in W1 and W8 have been obtained at the base temperature $T_b = 780$ K of the sample and are apart from the better statistics of W8 identical. Within time window W2 the sample is heated from the base temperature to some 100 K above the melting point ($T_m = 1828$ K). The third spectrum measured in W3 corresponds to the highest sample temperature and has been obtained entirely in the liquid state. We note that the shape of the valence band spectrum changes considerably at the phase transition. The main changes are the shift of the maximum intensity from 2 eV to 0.8 eV and the formation of a weak shoulder near 2.5 eV. The spectra measured in time windows W4–W7 reveal a gradual change towards the spectrum obtained at the base temperature (W8) associated with a gradual cooling of the sample surface.

Valence spectra from Nb, Ta, Mo and W have been obtained by the same technique. For each of these elements the spectrum measured at the base temperature in the solid state and the spectrum measured in the liquid state is shown for comparison in figure 3–6. Figure 3 shows the valence band spectra of Nb in the liquid state (bottom spectrum) obtained in time window W3 and two spectra measured in the solid state in time windows W5 and W8. From a fit of the Fermi–Dirac function at the Fermi edges information on the sample surface temperatures have been obtained with an accuracy of ± 150 K (see figure 3). It is evident from the spectra in figure 3 that almost no change takes place in the valence band spectrum at the solid–liquid phase transition with respect to the binding energy of the most intense peak at 0.6 eV and the should near 3 eV. However, after solidification a peak develops at a binding energy near 6 eV. This peak is already weakly visible in the high temperature spectrum in the solid phase measured 6 μs after the laser pulse and is fully developed in time window W8 measured 5 ms after the laser pulse. As we could show by time resolved XPS measurements, this 6 eV peak is associated with the formation of a surface oxide layer formed by the diffusion of oxygen from the bulk to the surface. This diffusion process is favoured by the high base temperature and is strongly reduced at lower base temperatures. It is important to note that the oxygen does not stem from the residual gas in the measuring chamber, since the ultra-high vacuum conditions are not influenced at all by the laser surface melting process. In fact, the pressure gauge does not show an increase in pressure during the laser irradiation. Similar surface oxidation effects have been observed in Ta and will be discussed elsewhere [24].

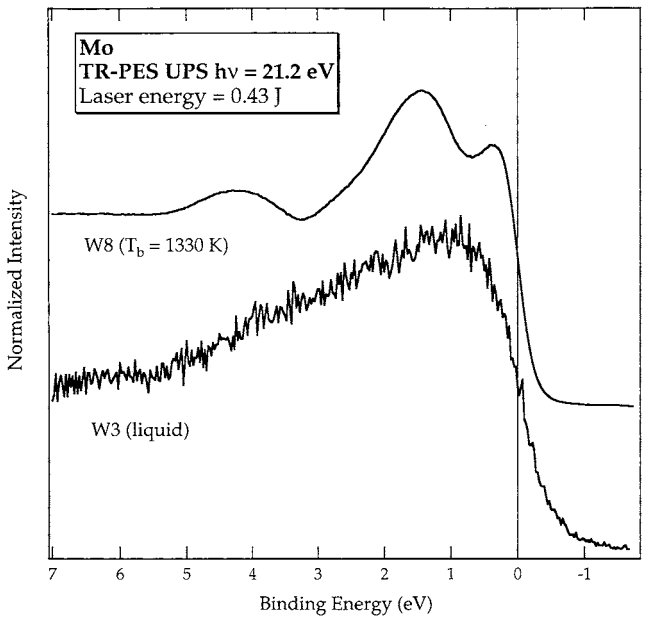

Figure 4. TR-PES valence band spectra of Mo: the liquid phase measured above the melting point of 2896 K and the solid phase measured at the base temperature of 1330 K.

A similar situation as in Nb can be found at the solid–liquid phase transition in Ta. Figure 5 shows the valence band spectra of liquid Ta measured above the melting point of 3290 K and the base temperature of 560 K. We note that the main features in the two spectra are very similar. The most intense peak is located close to the Fermi level and the shoulder near 3.5 eV is present in both spectra, though it is more intense in the solid phase. The steep onset in intensity near

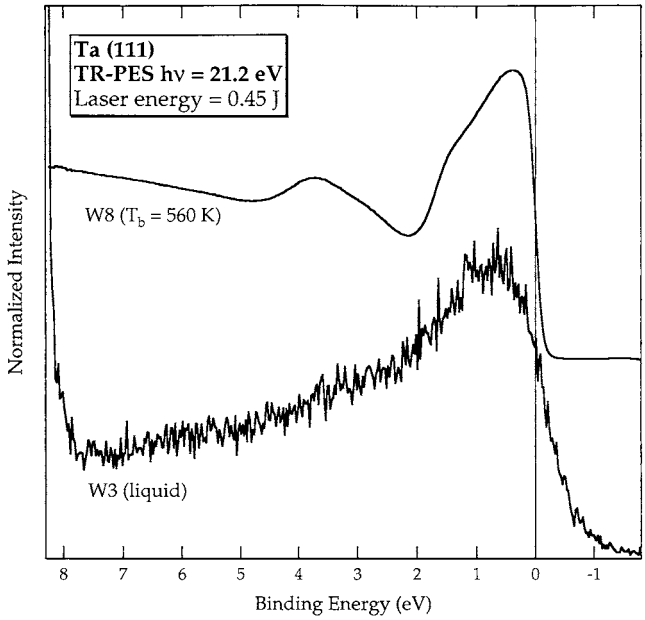

Figure 5. TR-PES valence band spectra of Ta: the liquid phase measured above the melting point of 3290 K and the solid phase measured at the base temperature of 560 K.

8 eV binding energy (which corresponds to an energy of $h\nu - E_B = 21.2 - 8$ eV $= 13.2$ eV above the Fermi level) is due to intense thermionic emission from the hot sample surface. This intense electron emission is responsible for the formation of a space charge above the sample surface which is most pronounced in three to four subsequent time windows after W3 and causes a reduction of photoelectron intensity. This effect will be discussed in more detail elsewhere [25].

Figure 4 shows the valence spectra of solid and liquid Mo. We note that the valence band of the solid phase measured at the base temperature of 1330 K reveals three peaks located at binding energies of 0.3, 1.4 and 4.1 eV. The valence band spectrum changes completely above the melting point of 2896 K. The separation of the band into two peaks at binding energies below 2 eV is no longer visible and one common structureless band is formed. The corresponding valence ban spectra of W are show in figure 6. The solid phase has been measured at the base temperature of 1220 K and the liquid phase spectrum has been obtained above the melting point of 3690 K. Again we note a complete change of the valence band spectrum at the phase transition. The two peaks located at 0.4 and 1.8 eV in the solid phase form one common band in the liquid phase and the peak at 5 eV is hardly visible in the liquid phase.

In short, the experimental results from five transition meals reveal (i) a distinct change of the valence band of Pd at the phase transition, (ii) only minor changes in the valence bands on melting for the group V transition metals Nb and Ta and (iii) marked changes in the valence band spectra of the group VI transition metals Mo and W. In addition, we note that surface oxidation effects occur at high base temperatures in Nb and Ta due to oxygen diffusion which can be studied by time resolved UPS and XPS with microsecond resolution. Due to intense thermionic emission, space charge effects occur which cause a general reduction in photoelectron intensity.

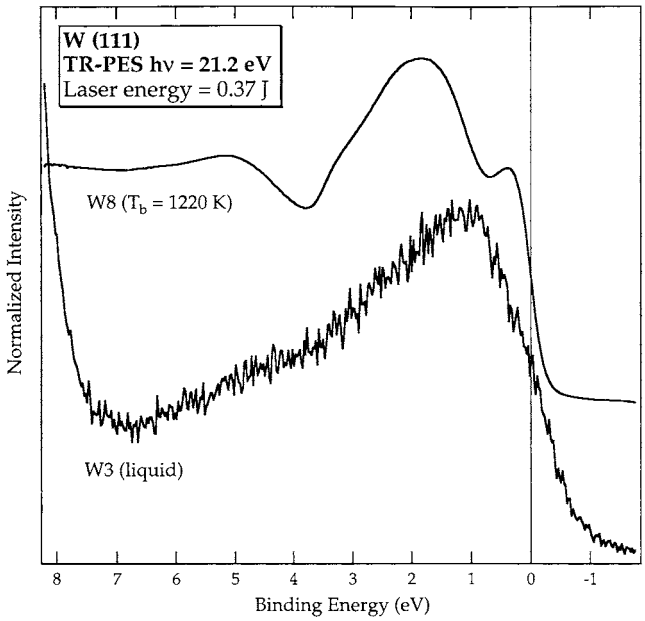

Figure 6. TR-PES valence band spectra of W: the liquid phase measured at 3700 K and the solid phase measured at the base temperature of 1200 K.

4. Discussion

4.1. Palladium

The valence band spectra across the solid (fcc) to liquid phase transition (figure 2) reveal distinct changes on melting. The question rises of whether these changes are associated with a change in the atomic short range order and, hence, with a change in the electronic structure of Pd on melting.

First we would like to stress that the valence band photoelectron spectra of a liquid phase can be interpreted on the basis of a weighted sum of the partial s, p and d electron density of states [11] since the excitation of photoelectrons is determined by energy conservation alone and, in contrast to the crystalline phase, $\boldsymbol{k}$-conservation is no longer an effective selection rule for the optical absorption process. The valence band spectra of crystalline Pd reveal rather strong changes as a function of the excitation energy in the UV range up to about $h\nu = 50$ eV due to direct optical transitions. The HeI excitation with $h\nu = 21.2$ eV yields a valence band spectrum with a distinct maximum near 2 eV binding energy (see the topmost curve in figure 2). For higher photon energies (>40 eV) the maximum is close to the Fermi level E_F [26] and the valence band spectrum resembles the total density of states [27]. A comparison of spectrum W3 obtained from liquid Pd (figure 2) with a density of states calculation for fcc Pd reveals a rather close similarity. Therefore, we do not interpret the changes in the valence band spectrum on melting on the basis of a change in the atomic short range order on melting but rather as a consequence of a change in the optical absorption process on melting from a $\boldsymbol{k}$-conservation dominated process to an absorption mechanism determined by energy conservation alone. Finally we would like to mention that the valence band spectrum of liquid Pd is in close agreement with a density of states calculation by Jank *et al* for liquid Pd [28].

4.2. Niobium, molybdenum, tantalum and tungsten

The UPS valence band spectra of *solid* Nb, Mo, Ta and W (which all crystallize in the bcc structure) measured with $h\nu = 21.2$ eV show a different behaviour than Pd. Their valence band spectra reveal features which can fully be explained on the basis of density of states calculations. This shows that the optical absorption process is determined by energy conservation alone and $\boldsymbol{k}$-conservation plays no dominant role.

Figures 3 to 6 show the valence band spectra of Nb, Mo, Ta and W across the solid–liquid phase transition. The group V elements Nb and Ta reveal almost no changes on melting (figures 3 and 5), whereas the group VI elements Mo and W show rather strong changes at the phase transition (figure 4 and 6). As mentioned above, in contrast to Pd, the valence band spectra of these transition metals reveal features which can clearly be associated with the density of states as we can see from a comparison with band structure calculations [29, 30]. The density of states calculations for Nb and Mo in the bcc and the hypothetical fcc structure by V L Moruzzi [29] are shown in figure 7. The valence band spectrum of solid Mo at 1330 K (upper curve in figure 4) reveals e.g. a minimum close to E_F, and two peaks close to 1.5 and 4 eV which can be associated with corresponding features in the density of states calculations if we admit that the two calculated peaks at 1.5 and 2.6 eV are not resolved in the valence band spectrum at 1330 K. Further we note that the densities of states of Nb and Mo are rather similar in both atomic structures (figure 7). The only marked difference is the position of the Fermi level of Nb and Mo, the latter with one more 4d electron per atom.

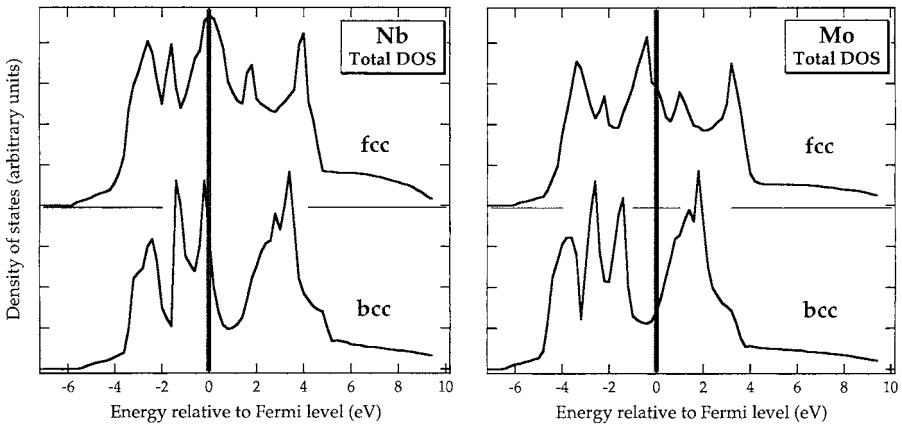

Figure 7. Calculated total density of states of Nb and Mo in the bcc and fcc structures [29].

Regarding the distinct changes in the valence band spectra of Mo and W on melting we suggest marked changes in the atomic short range order since we can exclude strong influences from a change in the photoemission process itself as in the case of Pd. As it turned out in earlier investigations on binary amorphous transition metal alloys [26, 31] the valence band spectra are best described by calculations for the fcc structure which did yield much better agreement than the bcc structure. Since the atomic structure of amorphous and liquid alloys are rather similar [11, 32] it is tempting to adopt the model of an fcc-like short range order for the liquid phases of Nb, Mo, Ta and W. Within this model the coordination number would be markedly increased on melting and the atomic short range order is fcc-like. A glance at figure 7 (or the density of states calculations for bcc and fcc W by Jansen and Freeman [30] or Davenport *et al* [33]) clearly shows why this change has only marked consequences for the valence bands of

Mo and W on melting: the deep minimum in the density of states of the bcc structure is filled up by a change towards an fcc-like short range order which is only visible in Mo and W since we only observe filled electron states in photoelectron spectroscopy.

5. Conclusion

Third generation photoelectron spectroscopy measurements which are not limited by vapour pressure limits have been applied to transition metals. Changes in the valence band spectra on melting have been associated with changes in the photoemission process in the case of Pd or with a distinct change in the atomic short range order on melting as in the case of Mo and W. We suspect a similar change in the short range order to occur in Nb and Ta. However, the densities of occupied electron states do not change so much as can be seen from corresponding band structure calculations and can therefore not be observed by photoelectron spectroscopy.

Acknowledgments

We acknowledge financial support of the Swiss National Science Foundation. Valuable assistance with numerical simulations has been provided by C Ellenberger and technical assistance by R Steiner is gratefully acknowledged. We acknowledge also the scanning electron microscopy picture by R Guggenheim and his collaborators.

References

[1] Berglund C N and Spicer W E 1964 *Phys. Rev.* A **136** 1030
[2] Spicer W E 1967 *Phys. Rev.* **154** 385
[3] Eastman D E 1971 *Phys. Rev. Lett.* **26** 1108
[4] Koyama R Y and Spicer W E 1971 *Phys. Rev.* B **4** 4318
[5] Enderby J E 1972 *Liquid Metals* ed S Z Beer (New York: Dekker) p 585
[6] Siegbahn K *et al* 1967 *Nova Acta Regiae Soc. Sci. Upsaliensis* Series IV, vol 20
[7] Indlekofer G, Oelhafen P and Güntherodt H-J 1987 *Physical and Chemical Properties of Thin Overlayers and Alloy Surfaces* vol 83, ed D M Zehner and D W Goodmann (Boston, MA: Materials Research Society) p 75
[8] Indlekofer G, Oelhafen P, Lapka R and Güntherodt H-J 1988 *Z. Phys. Chem., NF* **157** 465
[9] Indlekofer G, Oelhafen P, Güntherodt H-J, Hague C F and Mariot J M 1988 *Z. Phys. Chem. NF* **157** 575
[10] Oelhafen P, Indlekofer G and Güntherodt H-J 1988 *Z. Phys. Chem. NF* **157** 483
[11] Indlekofer G, Pflugi A, Oelhafen P, Güntherodt H-J, Häussler P, Boyen H-G and Bauman F 1988 *Mater. Sci. Eng.* **99** 257
[12] Indlekofer G and Oelhafen P 1989 *Disordered Systems and New Materials* ed M Borissov, N Kirov and A Vavrek (Singapore: World Scientific) p 707
[13] Indlekofer G, Pflugi A, Oelhafen P, Chauveau D, Guillot C and Lecante J 1990 *J. Non-Cryst. Solids* **117–8** 351
[14] Indlekofer G and Oelhafen P 1990 *J. Non-Cryst. Solids* **117–8** 340
[15] Pflugi A, Indlekofer G and Oelhafen P 1990 *J. Non-Cryst. Solids* **117–8** 336
[16] Indlekofer G and Oelhafen P 1991 *Synchrotron Radiation: Selected Experiments in Condensed Matter Physics* ed W Czaja (Basel: Birkhäuser) p 89
[17] Indlekofer G and Oelhafen P 1993 *J. Non-Cryst. Solids* **156–8** 226
[18] Gantner G, Boyen H-G and Oelhafen P 1995 *Europhys. Lett* **31** 163
[19] Gantner G, Boyen H-G, Oelhafen P and Rink K 1996 *J. Vac. Sci. Technol.* A **14** 2475
[20] Gantner G, Boyen H-G and Oelhafen P 1996 *J. Non-Cryst. Solids* **205–7** 490
[21] Stupp H, Boyen H-G, Gantner G and Oelhafen P 1996 *J. Phys.: Condens. Matter* **8** 9373
[22] Wahrenberg R, Stupp H, Boyen H-G and Oelhafen P 1999 *Europhys. Lett.* submitted
[23] Stupp H, Boyen H-G, Gantner G and Oelhafen P 1999 *J. Non-Cryst. Solids* at press
[24] Wahrenberg R, Oelhafen P and Stupp H 1999 to be published
[25] Oelhafen P Wahrenberg R and Stupp H 1999 to be published
[26] Oelhafen P 1987 *Amorphous and Liquid Materials (NATO Advanced Science Institute Series E: Applied Sciences 118)* ed E Lüscher, G Fritsch and G Jacucci, p 333

[27] Moruzzi V L 1985 *PhD Thesis* Technical University of Vienna
[28] Jank W, Hausleitner C and Hafner J 1991 *J. Phys.: Condens. Matter* **3** 4477
[29] Moruzzi V L 1984 Private communication
See also Moruzzi V L 1985 *PhD Thesis* Technical University of Vienna
[30] Jansen H J F and Freeman A J 1984 *Phys. Rev.* B **30** 561
[31] Oelhafen P 1983 *Glassy Metals II (Topics in Applied Physics 53)* ed H Beck and H-J Güntherodt (Berlin: Springer) p 283
[32] Häussler P, Indlekofer G, Boyen H-G, Oelhafen P and Güntherodt H-J 1991 *Europhys. Lett* **15** 759
[33] Davenport J W, Weinert M and Watson R E 1985 *Phys. Rev.* B **32** 4876